Improvement of Waveform for High Frequency AC-linked Matrix Converter with SVM based on Virtual Indirect Control

Kazuhiro Koiwa, and Jun-ichi Itoh

Department of Electrical engineering
Nagaoka University of Technology, NUT
Niigata, Japan
newkoiwa@stn.nagaokaut.ac.jp

Masashi Shioda

System Development Department
San-Eisha, Ltd.
Tokyo, Japan
shioda-masashi@san-eisha.co.jp

Abstract— **This paper proposes a dead-time compensation for a secondary side matrix converter with space vector modulation in order to improve waveform of the high frequency AC-linked matrix converter. The proposed system is constructed by back-to-back configuration of two three-phase to single phase matrix converters and a high frequency transformer. In order to improve the waveform, the dead-time compensation for the primary side matrix converter has been proposed. However, the dead-time compensation for the secondary side matrix converter with space vector modulation based on virtual indirect control has not been discussed. In this paper, the dead-time compensation method for the secondary side matrix converter is revealed. As the result, it is confirmed that the average output voltage error between the command and measured voltage is reduced by 20% at low modulation index by adopting the dead-time compensation. Finally, a 2-kW prototype is demonstrated by experiment. The efficiency and the input power factor at the maximum point were obtained by 91.4% and 0.997. Moreover, the input current total harmonic distortion (THD) is 5.65% at 2-kW output power.**

Keywords—high frequency linked matrix converter; dead-time compensation; space vector modulation

I. INTRODUCTION

Recently, the distributed power supplies which uses renewable energy source, such as wind turbine installed near the demand area are attracted. In such system, the commercial frequency transformers are used in terms of isolation and protection. However, the transformer at the commercial frequency is large [1].

In order to reduce the volume and weight of the transformer, the high frequency transformer system using back-to-back converter system, which consists of a PWM rectifier, a high frequency inverter, a high frequency rectifier, and a PWM inverter, has been discussed. Nevertheless, this system is bulky owing to boost-up inductor and the DC capacitor to smooth the DC link voltage. In addition, an efficiency of the system is low because the power conversion time is many.

On the other hand, the three-phase to single-phase matrix converter, has been proposed [2]-[6]. In this system, the advantages are the reduced size and long lifetime owing to the absence of an electrolytic capacitor and a boost-up inductor in comparison with the aforementioned back-to-back converter system. It is expected that the matrix converter is applied in renewable energy system such as wind power generation [7]-[9]. Moreover, the carrier comparison modulation is adopted in this system [2].

However, according to the modulation method in [2], the number of switching during one carrier period is not optimized. On the other hand, a space vector modulation based on a virtual indirect control method has been introduced for the control strategy of the primary matrix converter [3]. The features of this control method are as follows: (i) the reduced number of switching in comparison with [2], (ii) simple control strategy, and (iii) a zero vector can be equally distributed during one control period.

The authors proposed to adopt the space vector modulation based on the virtual indirect control method for the secondary side matrix converter previously [10]. Nevertheless, the commutation is required in an AC-AC direct converter. In particular, the dead-time error owing to commutation causes the input current distortion and the degradation of the output voltage control performance. The dead-time compensation for the primary side matrix converter has been discussed in order to improve the waveforms [3]. However, the dead-time compensation has not been adopted for the secondary side matrix converter.

In this paper, the dead-time compensation method for the secondary side matrix converter is proposed to improve the waveforms and the output voltage control performance. The dead-time error of the secondary matrix converter depends on the sign of the output current and the vector area of the output voltage command. Thus, it is necessary to change the dead-time compensation value by the sign of the output current and the output voltage command area.

The remainder of this paper is organized as follows. In section II, the circuit structure and features of the conventional system and proposed system are described. In section III, control strategies for the primary and secondary side matrix

converter are introduced. Then, the compensation method for the duty command of the secondary side matrix converter is referred to. In section IV, the dead-time compensation method for the secondary side matrix converter is explained and evaluated by simulation. Finally, the fundamental operation of the proposed system is demonstrated at 2-kW output power in experiment in section VI. In particular, the feasibility of the dead-time compensation method for the secondary side matrix converter is revealed by the experimental results.

II. CIRCUIT TOPOLOGY

A. Conventional high frequcency AC-linked converter

Fig. 1 shows a conventional back-to-back converter system. This system is composed of a PWM rectifier, a single phase high frequency inverter, a high frequency transformer, a high frequency rectifier, and a PWM inverter. The size of the transformer can be reduced in comparison with a commercial transformer. Nevertheless, this system is bulky owing to boost-up inductor and the DC capacitor to smooth the DC link voltage. In addition, the efficiency of this system is low because the power conversion time is many.

B. High frequency AC-linked matrix converter

Fig. 2 shows a proposed circuit using three-phase to single phase matrix converter and high frequency transformer. The proposed system can achieve high efficiency because the power conversion time is reduced in comparison with the conventional back-to-back converter system. Moreover, the volume and weight of the system are reduced owing to the absence of the electrolytic capacitor. For the reason, it is expected that the proposed system is applied to renewable energy fields such as a wind power conversion system.

III. CONTROL STRATEGY

Fig. 3 shows the control strategy of the proposed system. The single leg modulation is applied to primary side matrix converter control. On the other hand, in order to suppress the ripple current owing to the primary side matrix converter, the ripple compensation is applied to secondary side matrix converter control. In addition, the duty command T_{11}, T_{21} and T_{21}, T_{22} are calculated by space vector modulation based on virtual indirect control [11] [12]. However, the output voltage of the secondary matrix converter is distorted owing to the input voltage ripple. Thus, it is necessary to compensate the secondary duty command T_{21}, T_{22} by the primary duty command in duty conversion. Accordingly, the secondary duty command T_A, T_B, T_C and T_D are calculated from T_{11}, T_{12}, T_{21} and T_{22}. Next, the switching pulse is generated from the duty command and switching table. Finally, the pulse pattern of the primary matrix converter is decided by four-step voltage commutation [13]. On the other hand, the pulse pattern of the secondary matrix converter is decided by four-step or two-step current commutation.
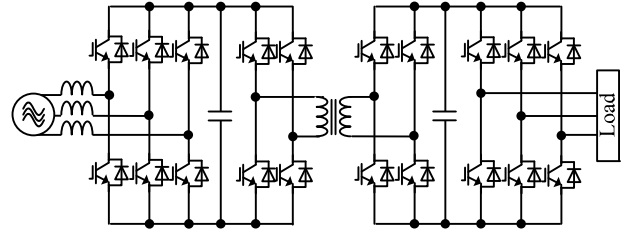
Fig. 1. Circuit configuration of conventional high frequency linked converter using high frequency transformer. This system has the large boost-up inductors and electrolytic capacitors as the drawbacks.
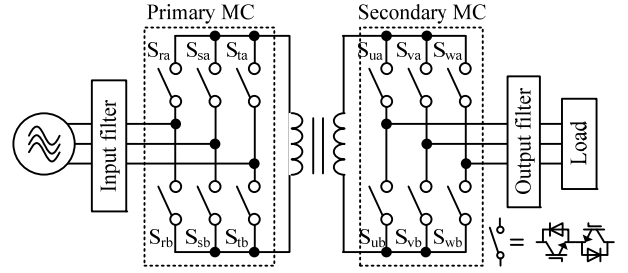
Fig. 2. Circuit configuration of high frequency AC linked matrix converter. The advantages of this system are high efficiency owing to less conversion time and the reduced size owing to absense of the boost-up inductor and electrolytic capacitor.
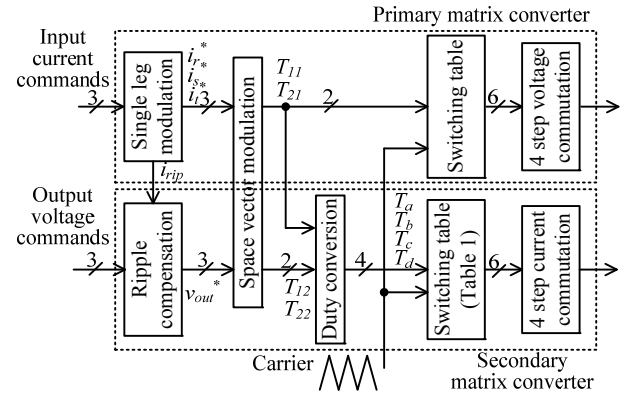
Fig. 3. Control block diagram of proposed system. A space vector modulation based on virtual indirect control is adopted. The duty commands of the secondary side matrix converter should be compensated by that of primary side matrix converter owing to input voltage ripple.

A. Virtual indirect control

The control strategy of the matrix converter is complicated. In order to control the matrix converter simply, virtual indirect control is applied [14] [15]. In virtual indirect control, the switching functions of the primary and secondary side matrix converters are expressed as

$$\begin{bmatrix} S_{ra} & S_{sa} & S_{ta} \\ S_{rb} & S_{sb} & S_{tb} \end{bmatrix} = \begin{bmatrix} S_{a1p} & S_{a1n} \\ S_{b1p} & S_{b1n} \end{bmatrix} \begin{bmatrix} S_{rp} & S_{sp} & S_{tp} \\ S_{rn} & S_{sn} & S_{tn} \end{bmatrix} \tag{1}$$

$$\begin{bmatrix} S_{ua} & S_{va} & S_{wa} \\ S_{ub} & S_{vb} & S_{wb} \end{bmatrix} = \begin{bmatrix} S_{a2p} & S_{a2n} \\ S_{b2p} & S_{b2n} \end{bmatrix} \begin{bmatrix} S_{up} & S_{vp} & S_{wp} \\ S_{un} & S_{vn} & S_{wn} \end{bmatrix} \qquad (2)$$

Note that S_{a1p}, S_{a1n}, S_{b1p}, and S_{b1n} are the switching function of the virtual inverter in the primary side matrix converter. S_{a2p}, S_{a2n}, S_{b2p}, and S_{b2n} are the switching function of the virtual rectifier in the secondary side matrix converter.

B. Primary side matrix converter

Fig. 4 shows the vector diagram of a virtual rectifier in the primary matrix converter. It is noted that the fundamental vectors and the pulse patterns are determined from the area of the input current command [3]. Furthermore, the switching duty T_{11}, T_{21}, and T_{z1} for the primary side matrix converter are expressed as

$$T_{11} = \frac{1}{|A|} \begin{vmatrix} v_\alpha & V_{2\alpha} \\ v_\beta & V_{2\beta} \end{vmatrix} \qquad (3)$$

$$T_{21} = \frac{1}{|A|} \begin{vmatrix} V_{1\alpha} & v_\alpha \\ V_{1\beta} & v_\beta \end{vmatrix} \qquad (4)$$

$$T_{z1} = 1 - (T_{11} - T_{21}) \qquad (5)$$

where v_α and v_β, are the output voltage command vector of α and β element, and $V_{1\alpha}$, $V_{1\beta}$, $V_{2\alpha}$ and $V_{2\beta}$ are fundamental vectors of the α and β element. Table I lists the switching table for the primary side matrix converter. The switching state for the virtual rectifier in (1) is decided from Table I.

On the other hand, the transformer voltage is generated by the virtual inverter. The switching function of the virtual inverter at the primary matrix converter is expressed as

$$\begin{bmatrix} S_{a1p} & S_{a1n} \\ S_{b1p} & S_{b1n} \end{bmatrix} = \begin{bmatrix} S_{a2p} & S_{a2n} \\ S_{b2p} & S_{b2n} \end{bmatrix} = \begin{cases} \begin{bmatrix} 0 & 1 \\ 1 & 0 \end{bmatrix} \\ \begin{bmatrix} 1 & 0 \\ 0 & 1 \end{bmatrix} \end{cases} \qquad (6)$$

The commutation is required in AC-AC direct converter. In particular, the dead-time error owing to commutation causes the input current distortion and the degradation of output voltage control performance [14].

Fig. 5 shows the relationship between the output voltage command for primary side matrix converter and the dead-time error. It is difficult to compensate the dead-time error, which depends on the sign of the output current for primary side matrix converter and the input phase voltage. However, the dead-time error is dominated by the amount of the switching duty [3]. Thus, the dead-time error for the primary side matrix converter can be compensated as
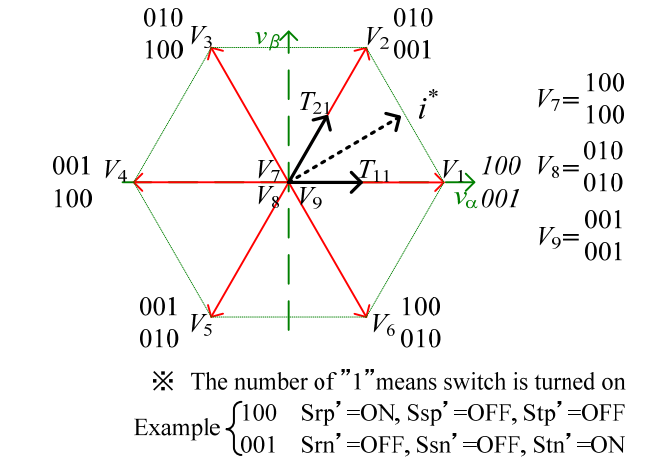
Fig. 4. Vector diagram of virtual indirect rectifier. The switching state is shown side of the vector. The uses of the vector V_1 and V_2 is selected from the area of the input current command.

TABLE I. SWITCHING TABLE FOR THE PRIMARY SIDE MATRIX CONVERTER.

	State	Area1	Area2	Area3	Area4	Area5	Area6
Positive	1	$V_1 = \frac{100}{001}$	$V_2 = \frac{010}{001}$	$V_3 = \frac{010}{100}$	$V_4 = \frac{001}{100}$	$V_5 = \frac{001}{010}$	$V_6 = \frac{100}{010}$
	2	$V_2 = \frac{010}{001}$	$V_3 = \frac{010}{100}$	$V_4 = \frac{001}{100}$	$V_5 = \frac{001}{010}$	$V_6 = \frac{100}{010}$	$V_1 = \frac{100}{001}$
	3	$V_8 = \frac{010}{010}$	$V_7 = \frac{100}{100}$	$V_9 = \frac{001}{001}$	$V_8 = \frac{010}{010}$	$V_7 = \frac{100}{100}$	$V_9 = \frac{001}{001}$
Negative	4	$V_5 = \frac{001}{010}$	$V_6 = \frac{100}{010}$	$V_1 = \frac{100}{001}$	$V_2 = \frac{010}{001}$	$V_3 = \frac{010}{100}$	$V_4 = \frac{001}{100}$
	5	$V_4 = \frac{001}{100}$	$V_5 = \frac{001}{010}$	$V_6 = \frac{100}{010}$	$V_1 = \frac{100}{001}$	$V_2 = \frac{010}{001}$	$V_3 = \frac{010}{100}$
	6	$V_7 = \frac{100}{100}$	$V_9 = \frac{001}{001}$	$V_8 = \frac{010}{010}$	$V_7 = \frac{100}{100}$	$V_9 = \frac{001}{001}$	$V_8 = \frac{010}{010}$

Fig. 5. Relationship between voltage command and dead-time error when the area of the input current command is "1" and the switching duty T_{21} is longer than T_{11}.

$$\begin{cases} T_{11}' = T_{11} \\ T_{21}' = T_{21} + T_{dead} \\ T_z' = 1 - (T_{11}' - T_{21}') \end{cases} , (T_{11} > T_{21}) \qquad (7)$$

$$\begin{cases} T_{11}' = T_{11} + T_{dead} \\ T_{21}' = T_{21} \\ T_z' = 1 - (T_{11}' - T_{21}') \end{cases} , (T_{11} < T_{21}) \qquad (8)$$

where T_{dead} is the dead-time compensation value.

C. Secondary side matrix converter

The switching duty T_{12}, T_{22}, and T_{z2} for the secondary side matrix converter are expressed as

$$T_{12} = \frac{1}{|A|} \begin{vmatrix} v_{o\alpha} & V_{o2\alpha} \\ v_{o\beta} & V_{o2\beta} \end{vmatrix} \tag{9}$$

$$T_{22} = \frac{1}{|A|} \begin{vmatrix} V_{o1\alpha} & v_{o\alpha} \\ V_{o1\beta} & v_{o\beta} \end{vmatrix} \tag{10}$$

$$T_{z2} = 1 - (T_{12} - T_{22}) \tag{11}$$

where v_α and v_β, are the output voltage command vector of α and β element, and $V_{1\alpha}$, $V_{1\beta}$, $V_{2\alpha}$ and $V_{2\beta}$ are fundamental vectors of the α and β element. However, the output voltage is distorted because the secondary side transformer voltage includes the difference voltage levels owing to the input voltage ripple. To solve this problem, it is necessary to compensate the on-duty command of the secondary side matrix converter.

Fig. 6 shows the duty compensation method for the secondary matrix converter. According to figure, T_a, T_b, T_c, T_d, and T_e which can divide to the several levels of output voltage of the secondary matrix converter, are expressed as

$$\begin{cases} T_a = T_{11} \times T_{12} \\ T_b = T_{11} \times T_{22} \\ T_c = T_{z2} \\ T_d = T_{21} \times T_{22} \\ T_e = T_{21} \times T_{12} \end{cases} \tag{12}$$

It is noted that T_{11}, T_{22} and T_{z2} are the duty command of the primary matrix converter. Additionally, d_a, d_b, d_c and d_d which is the duty command to obtain T_a, T_b, T_c, T_d, and T_e, are expressed as

$$\begin{cases} d_a = T_e + T_b + T_c + T_d \\ d_b = T_e + T_b + T_c \\ d_c = T_e + T_b \\ d_d = T_e \end{cases} \tag{13}$$

Finally, the pulse patterns of the secondary circuit are generated by comparing these duties with the carrier. Table II lists the switching table for secondary matrix converter. In this method, the average current becomes constant during the each control cycle. Moreover, secondary matrix converter control is synchronized with the primary circuit control.
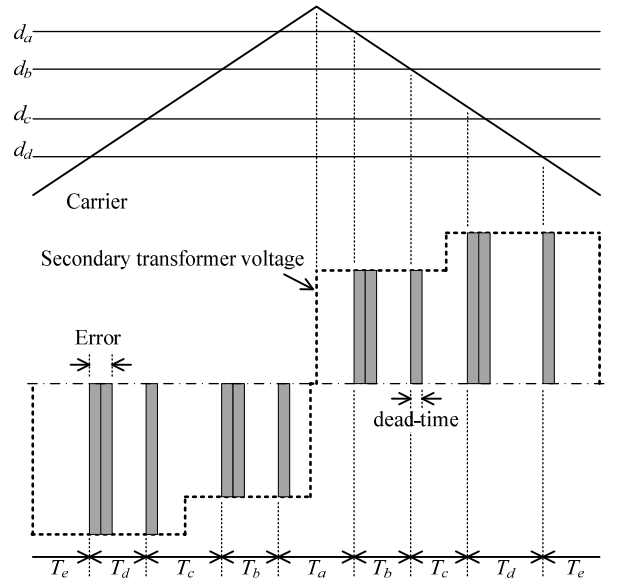
Fig. 6. The diagram of the carrier comparing modulation to control the secondary circuit and the dead-time error. The secondary transformer voltage (input voltage of secondary side matrix converter) includes the difference voltage level owing to input voltage.

TABLE II. SWITCHING TABLE FOR SECONDARY MATRIX CONVERTER.

	State		Area1	Area2	Area3	Area4	Area5	Area6
Positive	T_a	T_e	$V_1=\frac{100}{011}$	$V_2=\frac{110}{001}$	$V_3=\frac{010}{101}$	$V_4=\frac{011}{100}$	$V_5=\frac{001}{110}$	$V_6=\frac{101}{010}$
	T_b	T_d	$V_2=\frac{110}{001}$	$V_3=\frac{010}{101}$	$V_4=\frac{011}{100}$	$V_5=\frac{001}{110}$	$V_6=\frac{101}{010}$	$V_1=\frac{100}{011}$
	T_c		$V_7=\frac{111}{000}$	$V_0=\frac{000}{111}$	$V_7=\frac{111}{000}$	$V_0=\frac{000}{111}$	$V_7=\frac{111}{000}$	$V_0=\frac{000}{111}$
Negative	T_a	T_e	$V_4=\frac{011}{100}$	$V_5=\frac{001}{110}$	$V_6=\frac{101}{010}$	$V_1=\frac{100}{011}$	$V_2=\frac{110}{001}$	$V_3=\frac{010}{101}$
	T_b	T_d	$V_5=\frac{001}{110}$	$V_6=\frac{101}{010}$	$V_1=\frac{100}{011}$	$V_2=\frac{110}{001}$	$V_3=\frac{010}{101}$	$V_4=\frac{011}{100}$
	T_c		$V_0=\frac{000}{111}$	$V_7=\frac{111}{000}$	$V_0=\frac{000}{111}$	$V_7=\frac{001}{001}$	$V_0=\frac{000}{111}$	$V_7=\frac{111}{000}$

IV. DEAD-TIME COMPENSATION FOR SECONDARY SIDE MATRIX CONVERTER

The output voltage error owing to dead-time occurs according to Fig. 6. It is noted that the sign of U-phase and V-phase load current are positive, and the sign of W-phase load current is negative. In addition, the output voltage is DC voltage. Accordingly, the dead-time error is difference among each duty owing to the load current. Thus, in order to reduce the average output voltage, it is necessary to compensate the dead-time error from each duty and output current. For example, the dead-time compensation is expressed in Area1 as

$$\begin{cases} d_a{}' = d_a - T_{dead} \\ d_b{}' = d_b + T_{dead} \\ d_c{}' = d_c - T_{dead} \\ d_d{}' = d_d + T_{dead} \end{cases} \quad \begin{matrix} i_u > 0 \\ i_v > 0 \\ i_w < 0 \end{matrix} \tag{14}$$

$(Area1)$

where, T_{dead} is the dead-time compensation value. Similarly, it is necessary to compensate the dead-time in other Area and sign of output current. Table III lists the dead-time compensation value for the secondary side matrix converter. According to Table III, the dead-time compensation value is not dominated by one of the output currents. This is because one phase switch is not operated owing to space vector modulation.

V. SIMULATION RESULTS

In this chapter, the validity of the dead-time compensation for the secondary side matrix converter is revealed by simulation.

Fig. 7 shows the input and output waveforms of the proposed system without the dead-time in simulation. According to the result, the unity input power factor is obtained and the input current waveform is sinusoidal. In addition, it is confirmed that the proposed system can arbitrarily control the output frequency.

Fig. 8 shows the enlarged waveforms. In order to confirm the dead-time compensation for the secondary side matrix converter, the simulation results without the dead-time compensation and with dead-time compensation are shown in Fig. 8(a) and Fig. 8(b). According to Fig. 8(a), the output line voltage is generated from the input voltage of the secondary side matrix converter. Moreover, zero vector occurs when the secondary transformer voltage level is changed because the distortion of the output voltage is suppressed owing to input voltage ripple. On the other hand, in Fig. 8(b), it can be seen that the zero vector is not reduced because the dead-time compensation is adopted. Thus, the output voltage error between the output voltage command and real output voltage does not occur, and the degradation of the control performance for the output voltage is prevented.

Fig. 9 shows the average output voltage error characteristic against the modulation ratio in simulation in order to validate the dead-time compensation for secondary matrix converter. It is noted that the average output voltage with the dead-time compensation is compared with the output voltage, when there is no dead-time. Table IV lists the simulation parameters to confirm the validity of the dead-time compensation method for the secondary side matrix converter. As the result, the average output voltage error is reduced by 20% at low modulation ratio by adopting the dead-time compensation. Thus, it is expected that the control performance can be drastically improved at low modulation region.

Fig. 10 shows the output voltage ripple characteristics based on the modulation index. In lower modulation index, the output voltage ripple ratio without the dead-time compensation method is 19% owing to dead-time error. On the other hand, the output voltage ripple ratio with the dead-time compensation method is reduced by 2%. It is confirmed that the output voltage ripple is not reduced by the dead-time compensation. This is caused by the commutation error while next switching

TABLE III.   DEAD-TIME COMPENSATION VALUE FOR SECONDARY MATRIX CONVERTER.

Area	Sign of output current			Dead-time compensation value			
	i_u	i_v	i_w	d_a	d_b	d_c	d_d
Area1		+	+	$-T_{dead}$	$-T_{dead}$	$+T_{dead}$	$+T_{dead}$
		+	−	$-T_{dead}$	$+T_{dead}$	$-T_{dead}$	$+T_{dead}$
		−	+	$+T_{dead}$	$-T_{dead}$	$+T_{dead}$	$-T_{dead}$
		−	−	$+T_{dead}$	$+T_{dead}$	$-T_{dead}$	$-T_{dead}$
Area2	+	+		$+T_{dead}$	$+T_{dead}$	$-T_{dead}$	$-T_{dead}$
	+	−		$+T_{dead}$	$-T_{dead}$	$+T_{dead}$	$-T_{dead}$
	−	+		$-T_{dead}$	$+T_{dead}$	$-T_{dead}$	$+T_{dead}$
	−	−		$-T_{dead}$	$-T_{dead}$	$+T_{dead}$	$+T_{dead}$
Area3	+		+	$-T_{dead}$	$-T_{dead}$	$+T_{dead}$	$+T_{dead}$
	+		−	$+T_{dead}$	$-T_{dead}$	$+T_{dead}$	$-T_{dead}$
	−		+	$-T_{dead}$	$+T_{dead}$	$-T_{dead}$	$+T_{dead}$
	−		−	$+T_{dead}$	$+T_{dead}$	$-T_{dead}$	$-T_{dead}$
Area4		+	+	$+T_{dead}$	$+T_{dead}$	$-T_{dead}$	$-T_{dead}$
		+	−	$+T_{dead}$	$-T_{dead}$	$+T_{dead}$	$-T_{dead}$
		−	+	$-T_{dead}$	$+T_{dead}$	$-T_{dead}$	$+T_{dead}$
		−	−	$-T_{dead}$	$-T_{dead}$	$+T_{dead}$	$+T_{dead}$
Area5	+	+		$-T_{dead}$	$-T_{dead}$	$+T_{dead}$	$+T_{dead}$
	+	−		$-T_{dead}$	$+T_{dead}$	$-T_{dead}$	$+T_{dead}$
	−	+		$+T_{dead}$	$-T_{dead}$	$+T_{dead}$	$-T_{dead}$
	−	−		$+T_{dead}$	$+T_{dead}$	$-T_{dead}$	$-T_{dead}$
Area6	+		+	$+T_{dead}$	$+T_{dead}$	$-T_{dead}$	$-T_{dead}$
	+		−	$-T_{dead}$	$+T_{dead}$	$-T_{dead}$	$+T_{dead}$
	−		+	$+T_{dead}$	$-T_{dead}$	$+T_{dead}$	$-T_{dead}$
	−		−	$-T_{dead}$	$-T_{dead}$	$+T_{dead}$	$+T_{dead}$
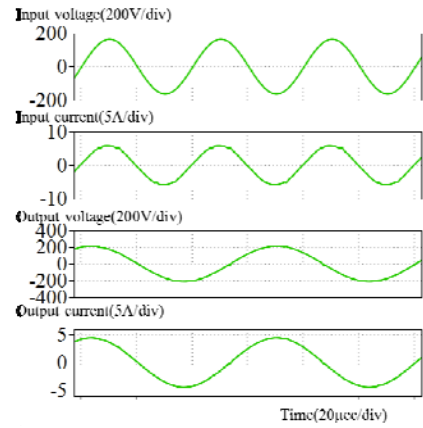
Fig. 7.   Operation waveforms of the proposed system without dead-time in simulation. From the top of figure, the input voltage, input current, output voltage (LPF), and output current are shown. In order to confirm that the output frequency can be changed, the output frequency is set to 30 Hz.

is interrupted into current commutation [15]. In order to reduce the output voltage ripple, it is necessary to improve the commutation patterns.

(a) without dead-time compensation

(b) with dead-time compensation
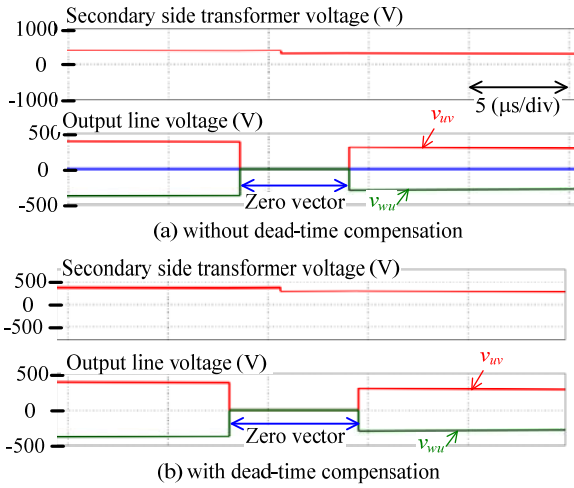
Fig. 8. Enlarged waveforms without dead-time compensation and with dead-time compensation for secondary side matrix converter. The dead-time is set to 1us. The primary side matrix converter is operated without the dead-time.

VI. EXPERIMENTAL RESULTS

Finally, similar to the simulation results, the fundamental operation of the proposed system and the feasibility of the dead-time compensation for the secondary side matrix converter are revealed by experiment.

Fig. 11 shows the operation waveforms of the proposed system at 2-kW output power by experiment. Table V lists the experimental conditions. A RL-load is used as the load. It is noted that the input and output voltage are 200 V, the dead-time compensation for the secondary matrix converter is not adopted. In Fig. 11 (a), the input current waveform is distorted. This is because the voltage commutation is adopted to the primary side matrix converter. Thus, the short circuit occurs in the primary side matrix converter by detection error of the input voltage. In order to solve this commutation problem, the hybrid commutation, which combines the voltage commutation with the current commutation, is adopted [13].

Fig. 11(b) shows the enlarged waveforms in the steady state by experiment. It is noted that the sign of the output voltage command is used instead of the output current in order to adopt the current commutation in the secondary side matrix converter. Similar to the simulation result, in order to suppress the output voltage ripple owing to difference level of the secondary side transformer voltage, the zero vector occurs. However, the zero vector has delay owing to dead-time. Furthermore, when the sign of the secondary side transformer voltage is changed, the negative output line voltage occurs. This is because of the dead-time error of the primary side matrix converter. The primary side transformer voltage is not zero because the current flows in free-wheeling diode. Moreover, the input power factor is almost unity and the input current waveform is sinusoidal. Thus, the fundamental operation at rated power is confirmed by experiment.
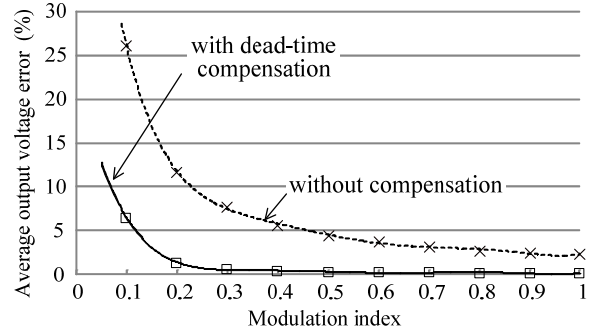
Fig. 9. Average output voltage error characteristic against modulation ratio in simulation. The average output voltage error is reduced with the dead-time compensation for secondary side matrix converter. In particular, as modulation index is 0.1, the average output voltage error is reduced by 20%.

TABLE IV. CALCULATION PARAMETERS FOR SECONDARY SIDE DEAD-TIME COMPENSATION.

Input line voltage V_{in} (V)	200	Output phase offset θ_o (rad/s)	0.7
Output line voltage V_{out} (V)	200	Area of output voltage command.	1
Output current I_o (A)	10	Dead-time d_{dead} (μs)	1.0
Output frequency f_{out} (Hz)	0	Dead-time comp. value T_{dead}	0.01
Switching frequency f_s (kHz)	10	Commutation method	4-step Current
Turn ratio of transformer	1.5	Transformer	Ideal
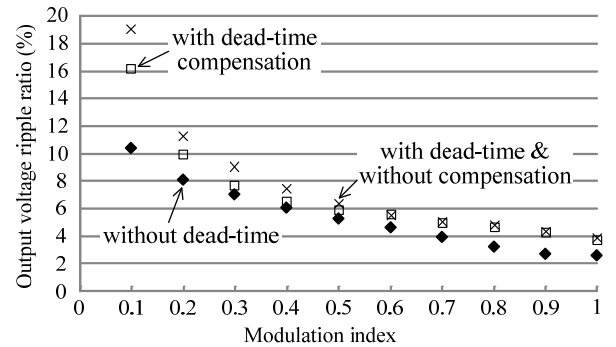
Fig. 10. Output voltage ripple characteristics based on modulation index. The output voltage ripple is not reduced with the dead-time compensation method. This is because the dead-time error is changed when next switching is interrupted into current commutation.

TABLE V. EXPERIMENTAL CONDITIONS.

Input line voltage V_{in} (V)	200	Input inductance (mH)	2.0
Output line voltage V_{out} (V)	200	Filter capacitance C_f (μF)	12.6
Modulation index m_o	0.866	Dead-time d_{dead} (μs)	1.0
Output frequency f_{out} (Hz)	30	Dead-time comp. value T_{dead}	0.01
Switching frequency f_s (kHz)	10	Commutation method	4-step Current
Turn ratio of transformer	1.2	Snubber resistance R_{snu} (kΩ)	44
Exciting inductance L_m (mH)	8.57	Leak inductance L_{leak} (μH)	3.18
Flux density B_m (Wb/m^2)	0.3	Current density J (A/mm^2)	3.0

Fig. 11(c) shows the spectrum of the input current at rated output power. According to the result, the large harmonic component of the input current does not occur owing to the input phase voltage ripple. Thus, it is confirmed that the duty command of the secondary side matrix converter can be compensated by the input voltage ripple.

Fig. 12 shows the efficiency and input power factor characteristics for the output power. The dead-time compensation is adopted in the secondary side matrix converter. Accordingly, the efficiency and input power factor at the maximum point are 91.4% and 0.997, respectively. In particular, the switching loss of the secondary side matrix converter dominates the converter efficiency. This is because the switching time of the secondary side matrix converter is twice of the primary side matrix converter, and the input voltage of the secondary one is higher owing to the transformer. In addition, all of the switching is the hard switching. Thus, to increase the efficiency of the proposed system, zero voltage switching is adopted to the secondary side matrix converter.

Fig. 13 shows the input current THD characteristic. It is noted that the dead-time compensation is applied to only primary side matrix converter. According to the result, it is accomplished that the input current THD is 6% or less. Thus, the proposed circuit can be connected to a grid owing to low input current THD. However, the input current THD is increased when the output power increases. This is caused by the dead-time error of the secondary side matrix converter. For this reason, it is necessary to compensate the dead-time error to reduce the harmonic components all of region.

Based on these results, the fundamental operation and validity of the dead-time compensation for the secondary side matrix converter can be revealed. It is expected that the control performance of the output voltage is improved by the dead-time compensation method.

VII. CONCLUSION

This paper proposed the dead-time compensation for a secondary side matrix converter in high frequency AC linked matrix converter with a space vector modulation based on virtual indirect control. The dead-time error of the secondary side matrix converter depends on the output voltage command area and the sign of the output current. Moreover, the dead-time compensation value is not dependent on one of the output current. This is because one phase switch is not operated owing to space vector modulation. Based on the conditions, it was necessary to compensate the dead-time error for the secondary side matrix converter. As the result, the average output voltage was improved by 20% at low modulation index by adopting the dead-time compensation in the simulation.

Furthermore, a 2-kW prototype of the high frequency AC linked matrix converter was demonstrated by experiment. It was confirmed that unity power factor and sinusoidal waveform of the input current are obtained. In particular, the input current THD is 5.65% at 2-kW output power. Moreover, the efficiency and the input power factor at the maximum point were obtained by 91.4% and 0.997. On the other hand, the validity of the dead-time compensation was confirmed by
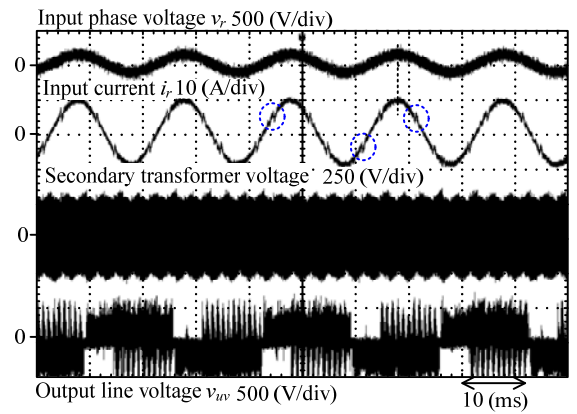
(a) Entire waveforms.
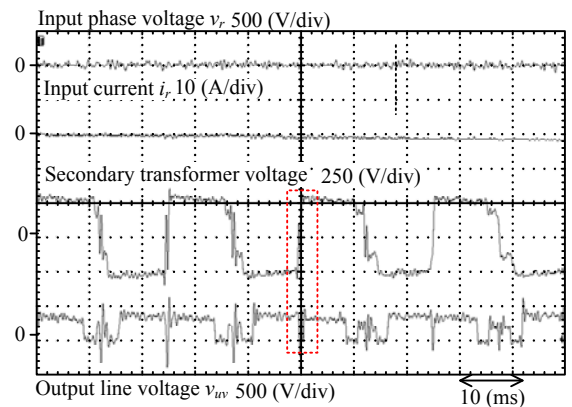
(b) Enlarged waveforms.
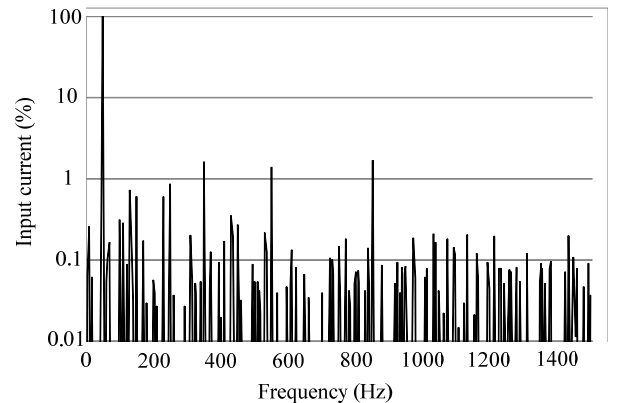
(c) Spectrum of input current.

Fig. 11. Fundamental operation of proposed system at rated power by experiment. In order to obtain 200-V output line voltage, the modulation index of the secondary side matrix converter is set to 0.86.

experiment in terms of reducing the average output voltage error. Accordingly , the average output voltage error could be reduced by adopting the dead-time compensation for the secondary side matrix converter. Thus, the dead-time compensation could improve the output voltage control performance.

In future works, the dead-time compensation for the secondary side matrix converter will be validated by experiment. Moreover, the total efficiency will be increased by

adopting a zero voltage switching for the secondary side matrix converter.

REFERENCES

[1] Harada, K., Anan, F., Yamasaki, K., Jinno, M., Kawata, Y., Nakashima, T.: "Intelligent transformer", Power Electronics Specialists Conference, 1996. PESC '96 Record., 27th Annual IEEE, Vol. 2, No. , pp. 1337-1341 (1996)

[2] J. Itoh, T. Iida, A. Odaka:" Realization of High Efficiency AC link Converter System based on AC/AC Direct Conversion Techniques with RB-IGBT" Industrial Electronics Conference, Paris, PF-012149,2006

[3] Goh Teck Chiang, K. Orikawa, Y. Ohnuma, J. Itoh: "Improvement of Output Voltage with SVM in Three-phase AC to DC Isolated Matrix Converter", IECON2013, (2013)

[4] Jin Aijuan, Li Hangtian, Li Shaolong: "A three-phase four-wire high-frequency AC link matrix converter for power electronic transformer", Electrical Machines and Systems, 2005. ICEMS 2005. Proceedings of the Eighth International Conference on, Vol. 2, No. , pp. 1295- 1300 (2005)

[5] Garces, A., Molinas, M.: "A Study of Efficiency in a Reduced Matrix Converter for Offshore Wind Farms", Industrial Electronics, IEEE Transactions on, Vol. 59, No. 1, pp. 184- 193 (2012)

[6] Han Ju Cha, Enjeti, P.N.: "A three-phase AC/AC high-frequency link matrix converter for VSCF applications", Power Electronics Specialist Conference, 2003. PESC '03. 2003 IEEE 34th Annual, Vol. 4, No. , pp. 1971- 1976 (2003)

[7] Young-Doo Yoon, Seung-Ki Sul: "Carrier-based Modulation Method for Matrix Converter with Input Power Factor Control and under Unbalanced Input Voltage Conditions", Applied Power Electronics Conference, APEC 2007 - Twenty Second Annual IEEE, Vol. , No. , pp. 310- 314 (2007)

[8] P. W. Wheeler, J. Rodriguez, J. C. Clare, L. Empringham: "matrix converters: A Technology Review" IEEE Transactions on Industry Electronics Vol. 49, No. 2, pp274-288, 2002.

[9] Diaz, M, Cardenas, R, Soto, G.: "4-wire Matrix Converter based voltage sag-swell generator to test LVRT in renewable energy systems", Ecological Vehicles and Renewable Energies (EVER),, Vol. , No. , pp. 1 - 10 (2014)

[10] Inoue, K., Shioda, M., Katade, M., Goto, A., Morishita, S., Itoh, J., Koiwa, K., "Space vector modulation based on virtual indirect control for high frequency AC-linked matrix converter," Power Electronics Conference (IPEC-Hiroshima 2014 - ECCE-ASIA), 2014 International (2014)

[11] J. Itoh, I. Sato, H. Ohguchi, K. Sato, A. Odaka, N. Eguchi: "A Control Method for the Matrix Converter Based on Virtual AC/DC/AC Conversion Using Carrier Comparison Method", IEEJ Trans. D, Vol. 124, No. 5, pp. 457-463 (2004)

[12] J. Itoh, H. Kodachi, A. Odaka, I. Sato, H. Ohguchi, H. Umida: "A High Performance Control Method for the Matrix Converter Based on PWM generation of Virtual AC/DC/AC Conversion", JIASC IEEJ, Vol. , No. , pp. I-303-I-308 (2004)

[13] K. Kato, J. Itoh: "Development of a Novel Commutation Method which Drastically Suppresses Commutation Failure of a Matrix Converter", IEEJ Trans. D, Vol. 127, No. 8, pp. 829-836 (2007)

[14] Terunuma, T., Konishi, Y., Takada, T., Matsuse, K.: "Compensation Method of Matrix Converter Drive System for commutation voltage
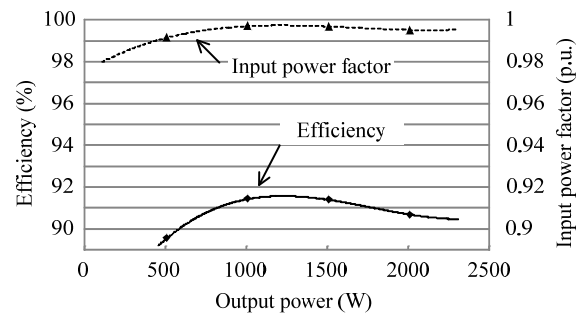
Fig. 12. Efficiency and input power factor characteristics for output power. The output voltage is 200V constantly by adjusting the modulation index
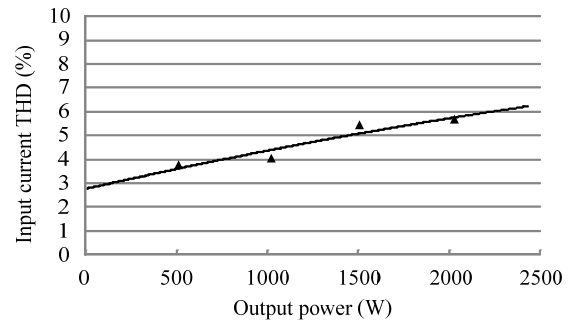
Fig. 13. Input current THD characteristic against output power. The input current THD is 5.65% at rated output power.

error and unbalanced input voltage", Industrial Electronics, 2009. IECON '09. 35th Annual Conference of IEEE, Vol. , No. , pp. 4505-4510 (2009)

[15] H. Hara, E. Yamamoto, J. K. Kang, T.J. Kume: "Improvement of Output Voltage Control Performance for Low Speed Operation of Matrix Converter", IEEE PESC, Vol. , No. , pp. 2910-2916 (2004)

[16] Ziegler, M., Hofmann, W.: "SEMI NATURAL TWO STEPS COMMUTATION STRATEGY FOR MATRIX CONVERTERS", Power Electronics Specialists Conference, 1998. PESC 98 Record. 29th Annual IEEE, Vol. 1, No. , pp. 727- 731 (1998)

[17] Bi He, Xingwei Wang, Hua Lin, Hongwu She: "Research on Two-step Voltage-controlled Commutation Strategies for Matrix Converter", Power Electronics and Motion Control Conference, 2009. IPEMC '09. IEEE 6th International, Vol. , No. , pp. 1745- 1751 (2009)

[18] Xingwei Wang, Hua Lin, Hongwu She, Bi He: "Implementation of Two-step Voltage Commutation Matrix Converter", Power Electronics and P. W. Wheeler, J. Rodriguez, J. C. Clare, L. Empringham: "matrix converters: A Technology Review" IEEE Transactions on Industry Electronics Vol. 49, No. 2, pp274-288, 2002.